Research Paper

DYNAMICAL ESTUARINE ECOSYSTEM MODELING OF PHYTOPLANKTON SIZE STRUCTURE USING STELLA

Bach Quang Dung[1]

ABSTRACT

An ecosystem model was developed for size-structured phytoplankton dynamics of coastal bay. State variables of the model include major inorganic nutrients ($NO_2^- + NO_3^-$, NH_4^+, PO_4^{3-}, Si), size classes of phytoplankton (microphytoplankton ($>20\mu m$), nanophytoplankton ($<20\mu m$), two classes of zooplankton (mesozooplankton, microzooplankton), and organic matters (POC, DOC). The iconographic interface of STELLA model was used to facilitate construction of the dynamic ecosystem model. The ecosystem model was integrated with STELLA 7.0 using a 4th order Runge-Kutta method (a numerical variable time step). The developed method suggested that the dynamical model using STELLA software can be useful to study phytoplankton dynamics in the pelagic coastal ecosystem.

Keywords: *Ecosystem model, Phytoplankton, Zooplankton, STELLA.*

1. Introduction

In microbial food web, the different sized phytoplankton can be affected differently by nutrient uptakes and light utilization as well as grazing in water column (Sin et al., 2000; Varela et al., 2005; Kriest and Oschlies, 2007; Chen et al., 2008). The growth of each phytoplankton size class is also different depending on seasons (Wilkerson et al., 2006; Marquis et al., 2007; Garcia et al., 2008; Weston et al., 2008).

In estuaries, the variability of plankton is associated with complex physical forcing including deterministic (tides), stochastic (wind, turbulence) components and nutrient enrichments (Allen et al., 2008; Lee et al., 2008; Pannard et al. 2008; Vallières et al., 2008). A better understanding of estuarine ecosystems becomes a key issue in environmental research for coastal waters as well as freshwater environments. Dynamical model is a useful tool for understanding plankton in estuarine coastal ecosystem (Flynn, 2005; Dube and Jayaraman, 2008; Rogachev et al., 2008). Size-structured phytoplankton dynamics were incorporated in estuarine coastal ecosystem model developed by Sin and Wetzel (2002).

The spring blooms were observed by many studies in coastal estuaries, major mechanisms of spring bloom included (1) high number of germinable diatoms in sediment during spring (Hansen and Josefson, 2003), (2) germination at the surface forced from resuspension of the sediment during winter mixing of the water column

✉ Bach Quang Dung
Corresponding author: dungmmu05@gmail.com
[1]Vietnam Journal of Hydrometeorology, Vietnam Meteorological and Hydrological Administration, Hanoi, Vietnam.

(Ishikawa and Furuya, 2004).

STELLA was developed as tool for ecological and economic system modeling (Costanza et al., 1998; Costanza and Gottlieb, 1998; Costanza and Voinov, 2001). STELLA was also applied for germination and vertical transport of cyst forming dinoflagellate model by Anderson (1998) and reservoir plankton system model by Angelini and Petrere (2000).

2. Methodologies
2.1 Model description

The ecosystem model includes 10 state variables (Fig. 1) nano- (< 20 μm), net- (> 20 μm) phytoplankton; microzooplankton (> 200 μm and < 330 μm), mesozooplankton (>330 μm); nutrients $NO_2^- + NO_3^-$, NH_4^+, PO_4^{3-} dissolved Si, and non-living organic materials, DOC and POC. Large and small phytoplankton are differentiated in their ability for nutrients, light limitations, temperature dependent metabolism and assimilation rate. Germination of netphytoplankton was considered together with wind forcing effect.
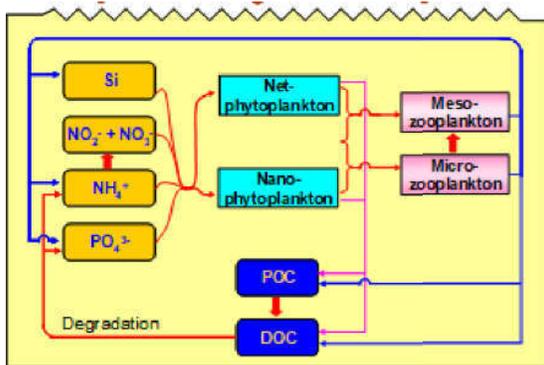
Fig. 1. The general scheme describing model structure for plankton in estuaries

The grazer variables were differentiated by the size structure of potential prey, as well as their half-saturation foods and assimilation rates (at 10°C) and affected by temperature response factor. POC, DOC were released from phytoplankton accumulation and zooplankton excretion and mortality. Nutrients were enriched by bacterial degradation of organic matter and grazer excretion. The ecosystem model was integrated with STELLA 7.0 using the function (a numerical variable time step differential equation solver using a 4th order Runge-Kutta method).

2.2 Mathematical structure of biological and chemical processes
Producers

Phytoplankton biomass (Phy) is determined by growth rate, germination rate (netphytoplankton), respiration rate, mortality rate and grazing rate (Tables 1-2).

Phytoplankton growth, G_P (Eq. 1) can be affected by assimilation rate at 10°C (ass), temperature response factor ( ), light limitation (f_L) and nutrient limitation (f_{NU}) and phytoplankton biomass (Phy) for each size-structure.

$$G_P = ass \cdot \tau \cdot f_L \cdot f_{NU} \cdot Phy \qquad (1)$$

Temperature response factor ( ) was presented by Blackford et al. (2004)

$$\tau = Q_{10}^{((Temp-10)/10)} - Q_{10}^{((Temp-30)/4)} \qquad (2)$$

Light limitation (f_L) in Eq. 3 (DiToro et al., 1971) is determined by f, k_d, z, I_m, I_o, where f is the photo-period, kd is light attenuation coefficient (m^{-1}), z is the depth (m), and I_m and I_o are incident average and optimal light (E m^{-2} d^{-1}), respectively. Light attenuation (k_d) was measured over the annual cycle. Daily k_d values were interpolated based on the field data.

Table 1. Symbol and unit for state variables

Variables	Symbol	Unit
Nanophytoplankton	NP	g C m^{-3}
Netphytoplankton	MP	g C m^{-3}
Microzooplankton	Z1	g C m^{-3}
Mesozooplankton	Z2	g C m^{-3}
Particulate organic carbon	POC	g C m^{-3}
Dissolved organic carbon	DOC	g C m^{-3}
Ammonium	N1	μM
Nitrite+nitrate	N2	μM
Orthophosphate	P	μM
Silicate	Si	μM

Table 2. Differential equations employed for 10 state variables

No.	Variable
1	Nanophytoplankton
	$\dfrac{dNP}{dt} = G_P - R_P - M_P - p \cdot G_Z$
2	Netphytoplankton
	$\dfrac{dMP}{dt} = G_P + G_{GM} - R_P - M_P - p \cdot G_Z$
3	Microzooplankton
	$\dfrac{dZ1}{dt} = G_Z - R_Z - M_Z - E_Z - L_Z$
4	Mesozooplankton
	$\dfrac{dZ2}{dt} = G_Z - R_Z - M_Z - E_Z - L_Z$
5	Particulate organic carbon
	$\dfrac{dPOC}{dt} = f_{Ez} \cdot \sum E_Z + f_{Mz} \cdot \sum M_Z + f_{Mp} \cdot \sum M_P - POC \cdot r_{hyd}$
6	Dissolved organic carbon
	$\dfrac{dDOC}{dt} = k_{Ez} \cdot \sum E_Z + k_{Mz} \cdot \sum M_Z + k_{Mp} \cdot \sum M_P + POC \cdot r_{hyd} - DOC \cdot r_{deg}$
7	Ammonium
	$\dfrac{dN1}{dt} = \left(DOC \cdot r_{deg} + \sum E_Z\right) / r_{C:N} - \left(Nitrif + \sum G_P\right) / r_{C:N}$
8	Nitrite+nitrate
	$\dfrac{dN2}{dt} = Nitrif + NO_{FW} - \left(\sum G_P\right) / r_{C:N} - L_{N2L}$
9	Ortho-phosphate
	$\dfrac{dP}{dt} = \left(DOC \cdot r_{deg} + \sum E_Z\right) / r_{C:P} - \left(\sum G_P\right) / r_{C:P} - L_{PB}$
10	Silicate
	$\dfrac{dS_i}{dt} = \left(POC \cdot r_{hyd} + \sum E_Z + \sum M_P\right) \cdot d_{Si} / r_{C:Si} - \left(\sum G_P\right) / r_{C:Si}$

$$f_L = \frac{e \times f}{k_d \times z} \left(e^{-\frac{I_m}{I_o} \cdot e^{-k_d z}} - e^{-\frac{I_m}{I_o}} \right) \qquad (3)$$

Monod (1942) model is applied for nutrient limitation f_{NU} (Eq. 4). The half-saturation constant (K_N) for nitrogen based on mean cell size (biovolume, μm3) is used Moloney and Field (1991) equations (Eq. 5). The half-saturation constant (K_P) for phosphorus is determined by dividing K_N by the N:P ratio (Eq. 5).

$$f_{NU} = MIN\left(\frac{N}{N + K_N}, \frac{P}{P + K_P}, \frac{Si}{Si + K_{Si}} \right) \qquad (4)$$

where K_N, K_P, K_{Si} are half-saturation constant of nutrients.

$$K_N = 2M^{0.38} \qquad K_P = \frac{K_N}{r_{N:P}} \qquad (5)$$

G_{GM} is germination enhancement incorporated for netphytoplankton. Germination is assumed by the maximum germination rate, wind mixing factor and germination potential over annual cycle in Eq. 6.

$$G_{GM} = r_{gm} \cdot W_{sp} \cdot p_{gm} \qquad (6)$$

where r_{gm} is the maximum germination rate, W_{sp} is wind mixing factor and pgm is germination potential (ranging from 0% to 100%).

Respiration of each size class is shown in (Eq. 7) by Blackford et al. (2004).

$$R_P = r_{BR} \cdot \tau \cdot Phy + (G_P - (G_P \cdot (f_{exu} + (1-a_N) \cdot (1-f_{exu}) \cdot r_{ar}) \qquad (7)$$

where r_{BR} is basal respiration of phytoplankton, f_{exu} is exudation under nutrient stress, a_N is nutrient limitation factor, r_{ar} is activity respiration.

$$M_P = r_{PM} \cdot Phy \qquad (8)$$

Phytoplankton mortality is described by Eq. 8

$$G_i = p \cdot G_Z \qquad (9)$$

where is mortality rate of phytoplankton
Loss of phytoplankton by grazer (Gi) is Eq. 9
where p is parameters describing the relative prey availability for each consumer, (Gz) is grazing by zooplankton.

Consumers

The zooplankton community including mesozooplankton, microzooplankton is considered. The consumer productions (Z) are determined by grazing, respiration, mortality, egestion and loss by predation (Tables 1-2).

Grazing of zooplankton is the uptake food from producers applied ERSEM model (Blackford et al., 2004) equation and described in Eq. 10.

$$G_Z = r_{Za} \times \tau \times F_{lim} \times Z \qquad (10)$$

where r_{Za} is zooplankton assimilation rate at 10ºC, (τ) is temperature response factor, Z is zooplankton biomass, F_{lim} is food limitation for grazers and described as

$$F_{lim} = \frac{f_Z}{f_Z + K_F} \qquad (11)$$

where K_F is half saturate food concentration.

$$f_Z = \sum_{F_Z=1}^{n} p \cdot F_Z \cdot \frac{F_Z}{F_Z + C_{minF}} \quad (12)(12)$$

where p is parameters of the relative prey for each consumer (described in Eq. 9), F_Z is biomass for each consumer, C_{minF} is lower threshold for feeding.

Respiration of zooplankton (R_Z) is shown in Eq. 13.

$$R_Z = r_{Basal} \cdot \tau \cdot Z + Gz \cdot (1 - eff_{ass}) \cdot (1 - f_{exc}) \quad (13)$$

where r_{Basal}, eff_{ass}, f_{exc} are basal respiration rate, efficiency of assimilation, fraction of excretion.

Mortality of zooplankton (MZ) is related to mortality rate (m_Z) and biomass of each zooplankton (Z) (Eq. 14).

$$M_Z = m_z \cdot Z \quad (14)$$

where m_z is mortality rate of zooplankton.

Zooplankton excretion is related to grazing (GZ), efficiency of assimilation ( ) and fraction of excretion f_{exc} in Eq. 15.

$$E_Z = Gz \cdot (1 - eff_{ass}) \cdot f_{exc} \quad (15)$$

LZ is loss of zooplankton by predation

$$L_Z = p_Z \cdot Z \quad (16)$$

where p_z is loss rate of each zooplankton by predation, Z is zooplankton biomass.

Organic matter

Particulate organic matter (POC) was expressed by supporting processes (POC_{sup}), (Eq. 17) and hydrolysis process (POC_{hyd}), (Eq. 18).

$$POC_{sup} = f_{Ez} \cdot \sum E_Z + f_{Mz} \cdot \sum M_Z + f_{Mp} \cdot \sum M_P \cdot \quad (17)$$

where f_{Ez} is fraction zooplankton excretion (E_Z) in POC; f_{Mz} is fraction zooplankton mortality (M_Z) in POC; f_{Mp} is fraction phytoplankton mortality (M_P) in POC.

$$POC_{hyd} = POC \cdot r_{hyd} \quad (18)$$

where r_{hyd} is hydrolysis rate of POC.

Dissolved organic matter (DOC) was ex-pressed by supporting processes (DOC_{sup}) (Eq. 19) and degradation process (DOC_{deg}) (Eq. 20).

$$DOC_{sup} = k_{Ez} \cdot \sum E_Z + k_{Mz} \cdot \sum M_Z + k_{Mp} \cdot \sum M_P + POC_{hyd} \quad (19)$$

where k_{Ez} is fraction zooplankton excretion (E_Z) in DOC; k_{Mz} is fraction zooplankton mortality (M_Z) in DOC; k_{Mp} is fraction phytoplankton mortality (M_P) in DOC.

$$DOC_{deg} = DOC \cdot r_{deg} \quad (20)(20)$$

where r_{deg} is degradation rate by heterotrophic bacteria.

Ambient Nutrients

Ammonium

Ambient ammonium was released by heterotrophic processes $\left[NH_4^+ \right]_{uptake}$ (Eq. 21) and uptake by nitrification process and phytoplankton growth $\left[NH_4^+ \right]_{uptake}$ (Eq. 22).

$$\left[NH_4^+ \right]_{in} = \left(DOC_{deg} + \sum E_Z \right) / r_{C:N} \quad (21)(21)$$

$$\left[NH_4^+ \right]_{uptake} = \left(Nitrif + \sum G_P \right) / r_{C:N} \quad (22)(22)$$

where $r_{C:N}$ is ratio carbon and nitrogen in biomass.

Nitrification process

The excretion processes produce ammonium and nitrification process converts ammonium to nitrite + nitrate (Jaworski et al., 1972).

$$Nitrif = [NH_4^+] \cdot e^{(k_t \times time)} \quad (23) \quad (23)$$

$$k_t = k_{20} \times \theta^{(temp-20)} \quad (24) \quad (24)$$

where k_{20} is nitrification rate at 20°C, θ is constant (1.188) for temperature adjustment of the nitrification rate.

Nitrite and nitrate

Ambient nitrite + nitrate was supplied by nitrification and freshwater input process, $\left[NO_2^- + NO_3^- \right]_{in}$ (Eq. 25) and uptake of phytoplankton, $\left[NO_2^- + NO_3^- \right]_{uptake}$ (Eq. 27).

$$\left[NO_2^- + NO_3^- \right]_{in} = Nitrif + NO_{FW} \quad (25)(25)$$

where NO_{FW} is nitrite+nitrate input from reshwater through embankments (Eq. 26).

$$NO_{FW} = e_{N2} \cdot TN_F \cdot per_{N2} \cdot (1 - Sal_{dif}) \quad (26)$$

where e_{N2} is efficiency for nitrite+nitrate input, TN_F is concentration of TN in freshwater input, per N_2 is percentage of nitrite+nitrate in freshwater TN, Sal_{dif} is salinity decrease factor.

$$\left[NO_2^- + NO_3^- \right]_{uptake} = \left(\sum G_P \right) / r_{C:N} + L_{N2L} \quad (27)$$

$$L_{N2L} = \left[NO_2^- + NO_3^- \right] \cdot r_{N2L} \quad (28)$$

where L_{N2L} is loss of nitrite + nitrate by bacterial uptake, $r_{C:N}$ is ratio carbon and nitrogen in biomass, r_{N2L} is loss rate of nitrite + nitrate by bacterial uptake.

Ortho-phosphate

Ortho-phosphate was related to processes such as excretion of zooplankton (E_Z) and bacterial degradation from DOC (DOC_{deg}) $\left[PO_4^{3-} \right]_{in}$ (Eq. 29) and phytoplankton uptake (GP) is $\left[PO_4^{3-} \right]_{uptake}$ (Eq. 30).

$$\left[PO_4^{3-} \right]_{in} = \left(DOC_{deg} + \sum E_Z \right) / r_{C:P} \quad (29)$$

$$\left[PO_4^{3-} \right]_{uptake} = \left(\sum G_P \right) / r_{C:P} + L_{PB} \quad (30)$$

$$L_{PB} = \left[PO_4^{3-} \right] \cdot r_{PL} \quad (31)$$

where L_{PB} is loss of orthophosphate by bacterial uptake; r_{PL} is loss rate of bacterial orthophosphate uptake; $r_{C:P}$ is ratio carbon and phosphorus in biomass.

Silicate

Silicate was obtained by POC hydrolysis (POC_{hyd}), excretion of zooplankton (E_Z), mortality of phytoplankton (M_P) in $\left[DS_i \right]_{in}$ (Eq. 32) and it was uptake by phytoplankton growth (G_P) $\left[DS_i \right]_{uptake}$ (Eq. 33).

$$\left[DS_i \right]_{in} = \left(POC_{hyd} + \sum E_Z + \sum M_P \right) \cdot d_{Si} / r_{C:Si} \quad (32)$$

where d_{Si} is dissolved S_i parameter from organic matter lysis.

$$\left[DS_i \right]_{uptake} = \left(\sum G_P \right) / r_{C:Si} \quad (33)$$

where $r_{C:Si}$ is ratio carbon and silic in biomass.

3. Results

3.1 Environmental change effect and predictions of model

Effects of temperature, attenuation coefficient and germination potential to size classes of phytoplankton by sensitivity analysis were observed in Fig. 2 to Fig. 6. The increase of temperature affected netphytoplankton in late spring. The increase enhanced nanophytoplankton in early spring and decreased them in late spring (Fig. 2). The change of attenuation coefficient (+10%) did not affect netphytoplankton, however nanophytoplankton were declined and total chl a decreased (Fig. 3).
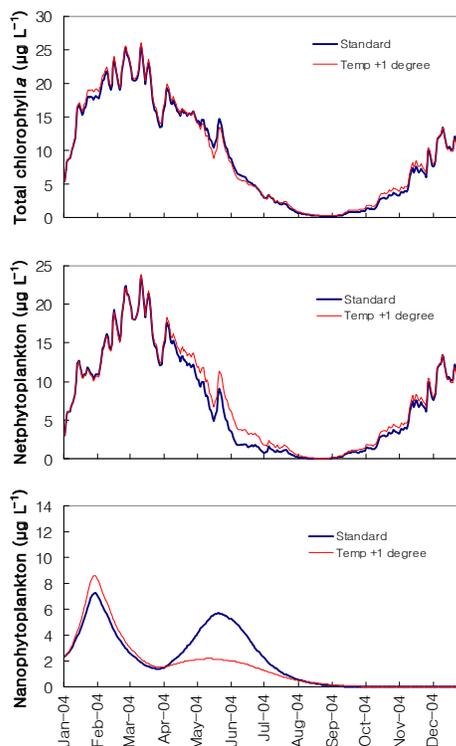
Fig. 2. Effect of temperature change to total chlorophyll a, net- and nanophytoplankton.

Germination potential has positive effect on netphytoplankton in cold season (winter and early spring) and total chl a concentration was increased during spring. Nanophytoplankton increased during late spring by enhancing germination potential (Fig. 4). P enrichment contributed to increase of nanophytoplankton as well as total chl a (Fig. 5). However, the combination of temperature (+ 1°C) attenuation coefficient (+10%) and P (+10%) reduced nanophytoplankton and enhanced netphytoplankton during late spring (Fig. 6).
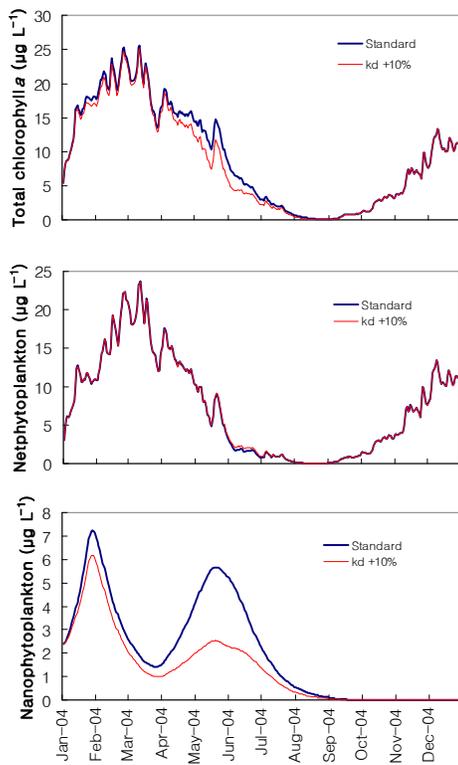
Fig. 3. Effect of attenuation coefficient change to total chlorophyll a, net- and nanophyto lankton

The annual mean percentage changes of state variables by changing environmental parameters were shown in Table 3. Nanophytoplankton were decreased with increase of temperature and attenuation coefficient. Netphytoplankton and nanophytoplankton were enhanced by increase of germination (Table 4). Nanophytoplankton were significant increase (30%) with increase of orthophosphate whereas netphytoplankton were insensitive to the change. Meso- and microzoo-

plankton responded negatively to the changes of temperature and attenuation coefficient. However, they responded positively to increases of germination potential and wind mixing and orthophosphate. POC and DOC were enhanced by increases in germination potential and wind mixing. Ammonium, orthophosphate and silicate were enhanced when temperature increased. Nitrite+nitrate was increased when salinity decreased.

3.2 Discussion

Size-based ecosystem models provide a simulation tool for understanding the structure and function of pelagic ecosystems. The ecosystem-based approach is also required to a range of environmental conditions. The variation of dynamics and community structures are produced by a variety of physical and chemical scenarios. The forcing factors defined by wind mixing, temperature, turbidity, germination potential, orthophosphate were used in the model.
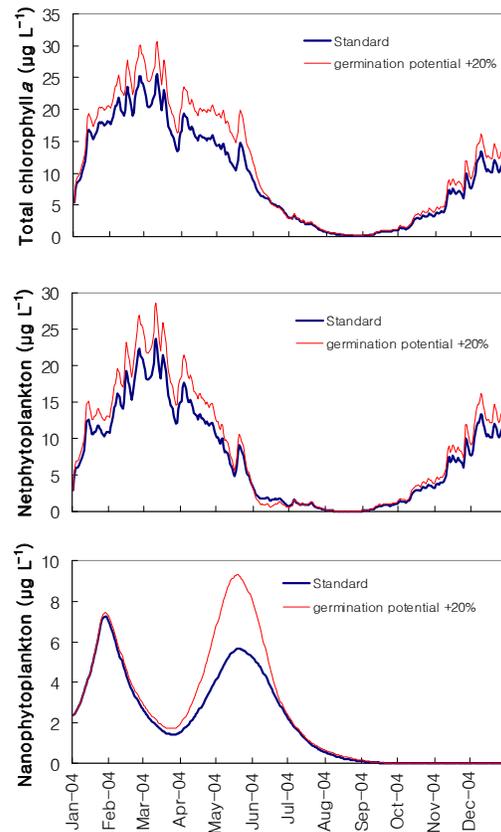
Fig. 4. Effect of germination potential change to total chlorophyll a, net- and nanophytoplankton
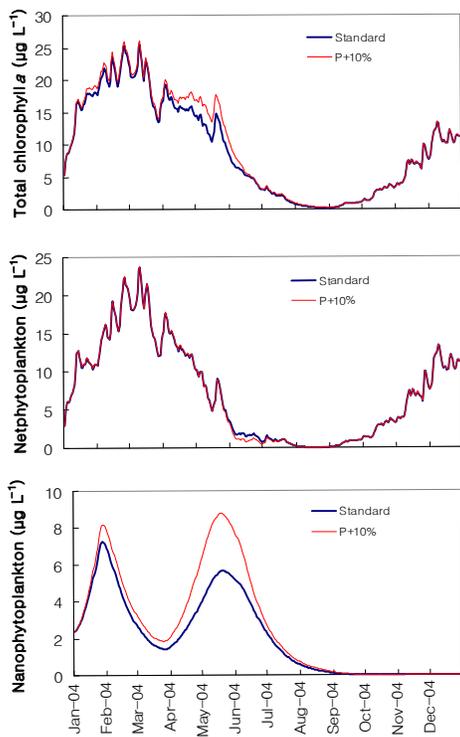
Fig. 5. Effect of phosphorus change to total chlorophyll a, net- and nanophytoplankton
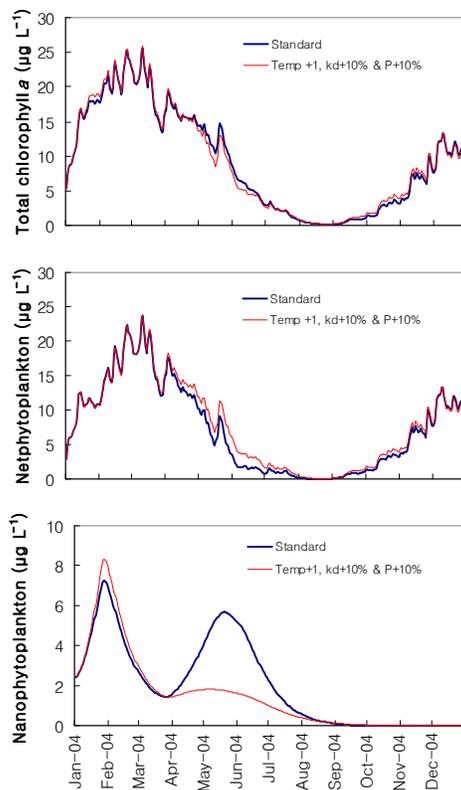
Fig. 6. Effect of temperature + attenuation coefficient + phosphorus change to total chlorophyll a, net- and nanophytoplankton

The simulation results showed a good agreement with ranges of observations suggesting that the model was plausibly linked to variations in mixing by wind, germination, temperature, turbidity and phosphorus supply.

The spring bloom period in each case is characterized by a succession of blooms, generally led by diatoms accounting netphytoplankton (data not shown). The diatom bloom was displayed over the seasonally maximum period of winter and early spring when wind speed increased. The wind mixing effect on phytoplankton (diatoms) germination at the surface during the cold season has been documented by Ishikawa and Furuya (2004). Diatom bloom such as Skeletonema costatum from resting stages occurred under wide range of water temperature in the coastal water (Shikata et al. 2008). Low temperature contributed to the spring bloom of diatoms (Andersson et al. 1994). In this model, netphytoplankton were dominant during early spring whilst nanophytoplankton dominated the production during late spring. The grazers exhibited a response after the spring bloom. Mesozooplankton and microzooplankton were typically responded to netphytoplanton bloom during spring.

The results of model simulations (Figs. 2-6) and sensitivity analysis (Table 4) demonstrated that the abiotic environmental parameters and variables: light, temperature, wind mixing, germination potential and orthophosphate play the major roles for phytoplankton dynamics in estuarine and coastal bay. The sensitivity analysis of ecosystem model showed that netphytoplankton are sensitive to change of wind mixing or germination potential, however nanophytoplankton were affected by not only these parameters but also by temperature, turbidity, and phosphorus. The size structures of phytoplankton were controlled by seasonality due to the wind mixing enhanced germination at the surface water from resting stage in the sediment. Phosphorus input also enhanced phytoplankton biomass, especially nanophytoplankton. It appeared that phosphorus could also drive phytoplankton growth and change in size structure of this ecosystem. The model could be useful to examine phytoplankton dynamics in relations to physical fac-

tors and nutrient dynamics.

4. Conclusion

Model validation for state variables suggested that the ecosystem model captures the phytoplankton and nutrient dynamics, and can be useful tool for analyses and management of an estuarine and coastal ecosystem which suffers nutrient enrichments and change of hydrology. The model also demonstrates that physical processes including wind mixing, water transparency, temperature as well as nutrients affect phytoplankton dynamics and response of phytoplankton can be related to the environmental changes in the coastal estuarine area.

Table 4. Results percentage change of sensitivity analysis for state variables given +1 degree change in temperature; -10% in salinity; +10% in attenuation coefficient, germination potential, wind speed, ammonium, nitrite+nitrate, orthophosphate, silicate. MP: netphytoplankton; NP: nanophytoplankton; Z_1: mircozooplankton; Z_2: mesozooplankton; DOC: dissolved organic matter; POC: particulate organic matter; N_1: ammonium; N_2: nitrite+nitrate; P: orthophosphate, S_i: silicate; –: % change <8%.

Parameters	State variables									
	MP	NP	Z_1	Z_2	DOC	POC	N_1	N_2	P	Si
Temperature +1ºC	–	-19.0	-66.3	-42.6	–	–	19.5	–	16.2	45.2
Attenuation coefficient k_d +10%	–	-34.3	-24.9	-19.7	–	–	–	–	–	35.2
Germination potential +10%	9.6	13.4	43.6	33.7	8.4	9.1	–	–	–	- 11.3
Salinity -10%	–	–	–	–	–	–	–	30.6	–	–
Wind speed +10%	9.6	13.4	43.6	33.7	8.4	9.1	–	–	–	-11.3
Ammonium +10%	–	–	–	–	–	–	12.7	–	–	–
Nitrite+nitrate +10%	–	–	–	–	–	–	–	10.3	–	–
Orthophosphate +10%	–	30.8	46.0	33.19	–	–	–	–	–	-35.3
Silicate +10%	–	–	–	–	–	–	–	8.9	–	13.6

References

1. Allen, J.I., Smyth, T.J., Siddorn, J.R., Holt, M., 2008. How well can we forecast high biomass algal bloom events in a eutrophic coastal sea? Harmful Algae, 8 (1): 70-76.

2. Angelini, R., Petrere, M., 2000. A model for the plankton system of the Broa reservoir, São Carlos, Brazil. Ecological Modelling, 126 (2-3): 131-137.

3. Anderson, J.T., 1998. The effect of seasonal variability on the germination and vertical transport of a cyst forming dinoflagellate, Gyrodinium sp., in the Chesapeake Bay. Ecological Modelling,112 (2-3): 85-109.

4. Andersson, A., Haecky, P., Hagström, Å., 1994. Effect of temperature and light on the growth of micro- nano- and pico-plankton: impact on algal succession. Marine Biology,120 (4): 511-520.

5. Blackford, J.C., Allen, J.I., Gilbert, F.J., 2004. Ecosystem dynamics at six contrasting sites: a generic modelling study. Journal of Marine Systems, 52 (1-4): 191-215.

6. Costanza, R., Duplisea, D., Kautsky, U., 1998. Ecological Modelling on modelling ecological and economic systems with STELLA. Ecological Modelling, 110: 1-4.

7. Costanza, R., Gottlieb, S., 1998. Modelling ecological and economic systems with STELLA: Part II. Ecological Modelling, 112 (2-3): 81-84.

8. Costanza, R., Voinov, A., 2001. Modeling ecological and economic systems with STELLA: Part III. Ecological Modelling, 143 (1-2): 1-7.

9. Chen, B., Liu, H., Wang, Z., 2008. Trophic interactions within the microbial food web in the South China Sea revealed by size-fractionation method. Journal of Experimental Marine Biol-

ogy and Ecology, 368 (1): 59-66.

10. Dominic, M.D.T., Donald, J.O., Robert, V.T., 1971. A Dynamic Model of the Phytoplankton Population in the Sacramento-San Joaquin Delta. Nonequilibrium Systems in Natural Water Chemistry, Chapter 5, 131-180.

11. Dube, A., Jayaraman, G., 2008. Mathematical modelling of the seasonal variability of plankton in a shallow lagoon. Nonlinear Analysis: Theory, Methods & Applications, 69 (3): 850-865.

12. Flynn, K.J., 2005. Modelling marine phytoplankton growth under eutrophic conditions. Journal of Sea Research, 54 (1): 92-103.

13. Garcia, V.M.T., Garcia, C.A.E., Mata, M.M., Pollery, R.C., Piola, A.R., Signorini, S.R., McClain, C.R., Iglesias-Rodriguez, M.D., 2008. Environmental factors controlling the phytoplankton blooms at the Patagonia shelf-break in spring. Deep Sea Research Part I, 55 (9): 1150-1166.

14. Hansen, J.L.S., Josefson, A.B., 2003. Accumulation of algal pigments and live planktonic diatoms in aphotic sediments during the spring bloom in the transition zone of the North and Baltic seas. Marine Ecology Progress Series, 248: 41-54.

15. Ishikawa, A., Furuya, K., 2004. The role of diatom resting stages in the onset of the spring bloom in the East China Sea. Marine Biology, 145 (3): 633-639.

16. Jaworski, N.C., Lear, D.W., Villa, O.J., 1972. Nutrient management in the Potomac Estuary, Nutrients and eutrophication, Specific Symposium American Society Limnology and Oceanography, 1: 246-367.

17. Kim, H.C., Yoo, S., Oh, I.S., 2007. Relationship between phytoplankton bloom and wind stress in the sub-polar frontal area of the Japan/East Sea. Journal of Marine Systems, 67 (3-4): 205-216.

18. Kriest, I., Oschlies, A., 2007. Modelling the effect of cell-size-dependent nutrient uptake and exudation on phytoplankton size spectra. Deep Sea Research Part I, 54 (9): 1593-1618.

19. Lee, D.I., Choi, J.M., Lee, Y.G., Lee, M.O., Lee, W.C., Kim, J.K., 2008. Coastal environmental assessment and management by ecological simulation in Yeoja Bay, Korea. Estuarine, Coastal and Shelf Science, 80 (4): 495-508.

20. Marquis, E., Niquil, N., Delmas, D., Hartmann, H. J., Bonnet, D., Carlotti, F., Herbland, A., Labry, C., Sautour, B., Laborde, P., Vézina, A., Dupuy, C., 2007. Inverse analysis of the planktonic food web dynamics related to phytoplankton bloom development on the continental shelf of the Bay of Biscay, French coast. Estuarine, Coastal and Shelf Science, 73 (1-2): 223-235.

21. Moloney, C.L., Field, J.G., 1991. The size-based dynamics of plankton food webs. I. A simulation model of carbon and nitrogen flows. Journal of Plankton Research, 13 (5): 1003-1038.

22. Pannard, A., Claquin, P., Klein, C., Roy, B.L., Véron, B., 2008. Short-term variability of the phytoplankton community in coastal ecosystem in response to physical and chemical conditions' changes. Estuarine, Coastal and Shelf Science, 80 (2): 212-224.

23. Rogachev, K.A., Carmack, E.C., Foreman, M.G.G., 2008. Bowhead whales feed on plankton concentrated by estuarine and tidal currents in Academy Bay, Sea of Okhotsk. Continental Shelf Research, 28 (14): 1811-1826.

24. Shikata, T., Nagasoe, S., Matsubara, T., Yoshikawa, S., Yoshikawa, Y., Shimasaki, Y., Oshima, Y., Jenkinson, I.R., Honjo, T., 2008. Factors influencing the initiation of blooms of the raphidophyte Heterosigma akashiwo and the diatom Skeletonema costatum in a port in Japan. Limnology and Oceanography, 53 (6): 2503-2518.

25. Sin, Y., Wetzel, R.L., 2002. Ecosystem modeling analysis of size-structured phytoplankton dynamics in the York River estuary, Virginia (USA). I. Development of a plankton ecosystem model with explicit feedback controls and hydrodynamics. Marine Ecology Progress

Series, 228: 75-90.

26. Vallières, C., Retamal, L., Ramlal, P., Osburn, C. L., Vincent, W.F., 2008. Bacterial production and microbial food web structure in a large Arctic river and the coastal Arctic Ocean. Journal of Marine Systems, 74 (3-4): 756-773.

27. Varela, M.M., Bode, A., Fernández, E., Gónzalez, N., Kitidis, V., Varela, M., Woodward, E.M.S., 2005. Nitrogen uptake and dissolved organic nitrogen release in planktonic communities characterised by phytoplankton size–structure in the Central Atlantic Ocean.

Deep Sea Research Part I, 52 (9): 1637-1661.

28. Weston, K., Greenwood, N., Fernand, L., Pearce, D.J., Sivyer, D.B., 2008. Environmental controls on phytoplankton community composition in the Thames plume, U.K.. Journal of Sea Research, 60 (4): 246-254.

29. Wilkerson, F.P., Lassiter, A.M., Dugdale, R.C., Marchi, A., Hogue, V.E., 2006. The phytoplankton bloom response to wind events and upwelled nutrients during the CoOP WEST study. Deep Sea Research Part II, 53 (25-26): 3023-3048.